Acta Oceanol. Sin., 2023, Vol. 42, No. 6, P. 112–120
https://doi.org/10.1007/s13131-022-2129-7
http://www.aosocean.com
E-mail: ocean2@hyxb.org.cn

Effects of *Ulva prolifera* dissipation on the offshore environment based on remote sensing images and field monitoring data

Longxiao Zheng[1], Mengquan Wu[1]*, Jie Zhao[2], Shaopeng Luan[2], Dongliang Wang[3], Wei Jiang[3], Mingyue Xue[1], Jiayan Liu[1], Yating Cui[1]

[1] College of Resources and Environmental Engineering, Ludong University, Yantai 264039, China

[2] Yantai Geographic Information Center, Yantai 264025, China

[3] Yantai Marine Environment Monitoring and Forecasting Center, Yantai 264040, China

Received 27 April 2022; accepted 12 October 2022

Abstract

Outbreaks of *Ulva prolifera* have continued in the South Yellow Sea of China (SYS) since 2007, becoming a serious marine ecological disaster. Large amounts of *U. prolifera* drift to the coast of the Shandong Peninsula to dissipate under the action of southeast monsoons and ocean surface currents. This causes serious harm to the ecological environment and economic activities of coastal cities. To investigate the impact of *U. prolifera* dissipation, this study extracted the spatiotemporal distribution of *U. prolifera* in the SYS from 2012 to 2020 based on the Google Earth Engine. The outbreak cycle of *U. prolifera* was determined by fitting analysis of outbreak time and coverage area through MATLAB. This study also looked at the effect of *U. prolifera* dissipation on water quality through field monitoring data. The results showed that the growth curve of the *U. prolifera* has a significant Gaussian distribution. The *U. prolifera* dissipates in Haiyang, China, in July and August every year and affects the offshore environment. Water quality parameters of seawater at different depths had significant differences after the *U. prolifera* dissipation. Changes in pH, chemical oxygen demand, nitrite nitrogen, nitrate nitrogen, ammonia nitrogen, chlorophyll *a*, total phosphorus, and suspended solids were more significant in surface seawater than in deeper water. Changes in the concentrations of dissolved oxygen and total nitrogen were more significant in the deep seawater (1.63 and 1.1 times higher than those in the surface seawater, respectively). The dissipation of *U. prolifera* releases a large amount of carbon and nitrogen into the seawater, which provides rich nutrients for phytoplankton and may cause secondary disasters such as red tide. These findings are useful for further understanding the rules of *U. prolifera* dissipation, as well as preventing and controlling green tide disasters.

Key words: *Ulva prolifera* dissipation, South Yellow Sea, Google Earth Engine, water quality, remote sensing

Citation: Zheng Longxiao, Wu Mengquan, Zhao Jie, Luan Shaopeng, Wang Dongliang, Jiang Wei, Xue Mingyue, Liu Jiayan, Cui Yating. 2023. Effects of *Ulva prolifera* dissipation on the offshore environment based on remote sensing images and field monitoring data. Acta Oceanologica Sinica, 42(6): 112–120, doi: 10.1007/s13131-022-2129-7

1 Introduction

Green tide is a marine ecological disaster caused by the rapid proliferation and accumulation of large amounts of *Ulva prolifera* under specific environmental conditions (Wu et al., 2014; Li et al., 2021a). The Brittany Coast of France (Schreyers et al., 2021), the Korean Peninsula (Kwon et al., 2017), and other countries and areas around the world have been affected by green tide for many years (Schreyers et al., 2021). It has become a striking recurrent ecological disaster in the South Yellow Sea of China (SYS) over the past 15 a (Wang and Wu, 2021). The outbreak of *U. prolifera* has had a significant negative impact on the local marine ecosystem and economy (Zhang et al., 2021c). The quantitative study of the dissipation effects of *U. prolifera* is essential to mitigate its economic and ecological losses.

Numerous studies have shown that the *U. prolifera* in the SYS drifts northward from the northern Jiangsu shoal of China in May and June each year and reaches the coast of Shandong Peninsula in July and August (Zhang et al., 2018; Sun et al., 2018). When the green tide enters the dissipation period, a large amount of *U. prolifera* begins to dissipate and release toxic substances, which affects the ecological environment of coastal cities (Li et al., 2021b). Many scholars have conducted studies on the influence of the dissipation of *U. prolifera*, including its effect on cultured abalone, sea cucumber (Wang et al., 2011), and phytoplankton (Xing et al., 2015). Green tide may lead to secondary disasters such as red tide (Kong et al., 2018). The most direct influence of the *U. prolifera* dissipation is change in the chemical environment of seawater (Li et al., 2021c). Therefore, many scholars have also conducted studies on this issue, including the water quality changes in nearshore waters (Zhang et al., 2020), the characteristic of nutrient release (Feng et al., 2020; Zhang et al., 2021b), and dissolved organic carbon changes during the long-term *U. prolifera* dissipation process (Chen et al., 2020). These studies have largely revealed the impact of *U. prolifera* dissipation on the

Foundation item: The National Natural Science Foundation of China under contract No. 42071385; the Shandong Natural Science Foundation under contract No. ZR2019MD041; the Open Project Program of Shandong Marine Aerospace Equipment Technological Innovation Center, Ludong University under contract No. MAETIC2021-12; the Yantai Science and Technology Innovation Development Plan Project under contract No. 2022MSGY062.
*Corresponding author, E-mail: ld_wmq@ldu.edu.cn

offshore environment. However, most of these studies have been conducted in the laboratory or have explored only numerical changes in water quality. The effects of *U. prolifera* dissipation on seawater at different depths is not known. Most of the existing studies describe the outbreak cycle of *U. prolifera* qualitatively (Sun et al., 2018). The dissipation period has been defined as the period of time from the date of outbreak until the date of dissipation (Li et al., 2021b). This method is easily affected by the temporal resolution of satellite images and effects of anomalous years, so it may not provide a representative long-term view of the *U. prolifera* outbreak cycle.

A *U. prolifera* outbreak is characterized by wide distribution, long duration, and macroscopic drift of the algae (Xing et al., 2015). The hyperspectral, large-scale, and dynamic nature of remote-sensing technology makes it uniquely suited for long-term series monitoring of a *U. prolifera* disaster. Traditional remote sensing is limited by the time-consuming and labor-intensive process of a large amount of data screening and processing, so it is difficult to monitor *U. prolifera* in the long-term and across sensors (Li et al., 2021b). The Google Earth Engine (GEE) platform solves this problem. GEE is a multi-source remote sensing image cloud computing platform supported by Google's Cloud Infrastructure (Hao et al., 2020). It can automatically visualize and analyze a large number of satellite images online by writing JavaScript code. The GEE platform has changed traditional remote sensing image processing and has been widely used in crop research (Yin et al., 2019), waterbody extraction (Nguyen et al., 2020), and other applications. However, large-scale monitoring of *U. prolifera* based on GEE has not been widely reported.

Based on the above analysis, this study used GEE and MATLAB fitting analysis to study *U. prolifera*. Curve models generated by Gaussian functions were used to determine the outbreak cycle of *U. prolifera*. Water quality data at different depths were used to analyze the impact of *U. prolifera* dissipation on the offshore environment along a vertical axis. In addition, this study investigated the effects of *U. prolifera* dissipation on the phytoplankton using polynomial fitting and mathematical analysis. The results of this study provide theoretical support for the early prevention and later control of green tide.

2 Materials and methods

2.1 *Study area*

The study area (Fig. 1) is located in the northern regions of the SYS (35°–37°N, 120°–122°E), which is a semi-enclosed shallow sea with an average depth of 44 m (Sun et al., 2018). It is located in a maritime monsoon climate zone with an average annual temperature of 14–20℃ (Zheng et al., 2022a). Major cities in the study area include Rizhao, Qingdao, and Haiyang, all in China. *Ulva prolifera* continues to have landfall in the southern waters of Haiyang since 2007. Haiyang is located in the northern part of the SYS on the southeastern Shandong Peninsula (36°16′–37°10′N, 120°50′–121°29′E) (Zhang et al., 2022b). It is an important sea cucumber farming base in China. However, the outbreak and dissipation of *U. prolifera* have seriously endangered the local farming activities and ecological environment.

2.2 *Data sources*

The satellite data used in this study are Landsat 7 ETM+ (GEEID: LANDSAT/LE07/C01/T1_SR), Landsat 8 OLI (GEEID: LANDSAT/LC08/C01/T1_SR), and Sentinel-2 MSI (GEEID: COPERNICUS/S2_SR) image data from 2012 to 2020 provided by the GEE. The Landsat satellites have a spatial resolution of 30 m and

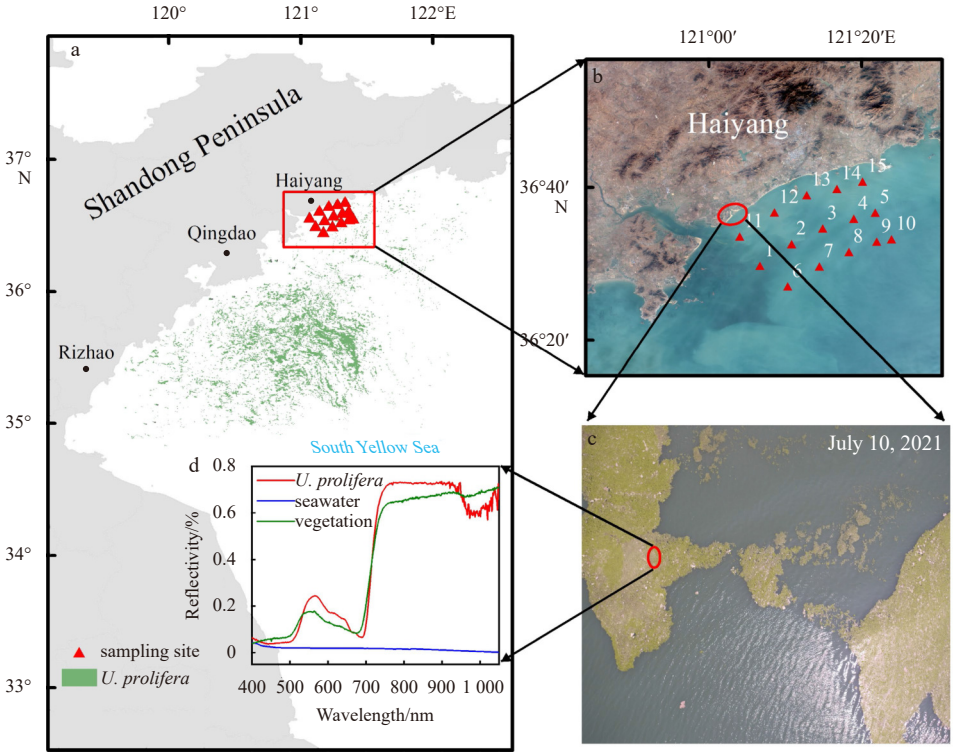

Fig. 1. Schematic of remote sensing for the effects of *Ulva prolifera* dissipation on the offshore environment in China (a); fifteen seawater sampling sites set up in June and August, 2020 in the Haiyang (b); *U. prolifera* floating in the sea, taken in Haiyang on July 10, 2021 (c); the spectral curves of *U. prolifera*, seawater, and vegetation (d).

a temporal resolution of 16 d. Sentinel-2 has a spatial resolution of 10 m and a temporal resolution of 5 d. Combining these two kinds of satellite images can reduce the influence of clouds, satellite spatial resolution, and other factors on information extraction.

The Surface Reflectance (SR) dataset provided by GEE is the atmospherically corrected surface reflectance. However, it does not remove clouds. We need to remove the clouds from the images because the high reflectivity of the clouds may reduce the accuracy of the *U. prolifera* extraction. We used the simple Cloud Score algorithm provided by the GEE to remove the clouds from Landsat images. The algorithm computes a simple cloud-likelihood score in the range [0, 100] using a combination of brightness, temperature, and normalized difference snow index. According to our experience, the threshold is set to 20 which can mask the cloud very well. We used Bitwise AND calculation to remove clouds of Sentinel-2 images. The bit 10 and bit 11 in the QA60 band in Sentinel-2 represent opaque clouds and cirrus clouds, respectively. In this study, we determined whether the bit 10 and bit 11 of the pixel are covered by clouds at the same time using Bitwise AND calculation. If clouds exist in both the bit 10 and bit 11 of the pixel, then the pixel is considered to be cloud, otherwise, the pixel is considered to be a valid pixel. Finally, the cloud pixels were masked to obtain the cloud-free image of Sentinel-2.

2.3 *Methods*

2.3.1 *Extraction of U. prolifera*

For the extraction of *U. prolifera*, we used the threshold segmentation method (Liu et al., 2009). First, the grayscale image was generated by band operation. Second, the grayscale image was binarized to distinguish the *U. prolifera* from the seawater. To distinguish *U. prolifera* from seawater on remote sensing images, we measured their spectral reflectance (Fig. 1d). According to the spectral curves (Fig. 1d), the spectral characteristics of *U. prolifera* are similar to those of terrestrial vegetation. The reflectance of *U. prolifera* was generally higher than that of the seawater. Therefore, we calculated the vegetation index to distinguish *U. prolifera* from seawater. The results show that normalized difference vegetation index (NDVI) can effectively extract *U. prolifera* in the presence of thin clouds and has the strongest detection ability for each growth stage of *U. prolifera* (Zhang et al., 2018, 2020). It distinguishes *U. prolifera* from seawater by normalizing the near-infrared and red bands. The formula for NDVI is as follows:

$$\mathrm{NDVI} = (\mathrm{NIR} - \mathrm{R})/(\mathrm{NIR} + \mathrm{R}), \tag{1}$$

where NIR represents the near-infrared band, and R represents the red band in visible light.

The key of the threshold segmentation method is the choice of threshold value. Many studies determine thresholds through experience or histogram methods that may be subjectively influenced by the researcher. This study calculated the maximum interclass variance of grayscale images by the Otsu algorithm on the GEE to automatically obtain the threshold value (Zhang et al., 2021a). First, the image pixels were divided into 0–255 levels by calculating the histogram of the image. The threshold T was set to start at 0 and iterate to 255. We defined pixels smaller than T as foreground and pixels larger than T as background. The percentage of foreground pixels to the entire image is p_0, and the average gray scale is g_0. The percentage of background pixels to the entire image is p_1, and the average gray scale is g_1. The mean gray scale of the image is g_2 and the interclass variance is F. The interclass variance F of the image was calculated by Eqs (2) and (3). T at the maximum interclass variance is the full image threshold.

$$g_2 = p_0 \times g_0 + p_1 \times g_1, \tag{2}$$

$$F = p_0(g_0 - g_2)^2 + p_1(g_1 - g_2)^2. \tag{3}$$

2.3.2 *Processing of water quality data*

We went to Haiyang of China twice (in June and August 2020) to collect seawater samples for water quality analysis. The collection dates represent times before and after the dissipation of *U. prolifera* (Table 1). We set up 3 sections in Haiyang with a total of 15 seawater collection points that cover the sea area affected by *U. prolifera* in Haiyang (Fig. 1b). Based on the *Technical Specification for Offshore Environmental Monitoring, Part 3 Offshore Seawater Quality Monitoring of China* (HJ 442.3–2020) and the actual situation of the sea, we collected 15 seawater samples of 0.1–1 m depth and 10 seawater samples of 1–10 m depth in each field survey.

Table 1. Basic conditions of seawater sampling sites

Sampling sites	Water depth/m	Sea surface temperature/℃		Wind speed/(m·s^{-1})		Transparency/m	
		June	August	June	August	June	August
1	8.0	25.2	28.6	7.2	4.9	1.1	6.0
2	8.2	25.0	29.0	4.9	3.8	1.4	2.5
3	8.4	24.6	28.8	1.9	4.1	1.7	2.5
4	7.8	23.9	28.4	4.2	4.0	0.8	2.0
5	8.3	24.0	28.4	4.5	4.8	1.0	1.0
6	8.2	24.4	28.4	6.4	5.8	1.2	7.0
7	10.1	24.0	28.2	4.4	5.5	2.0	4.5
8	11.4	24.2	28.2	3.2	4.6	2.9	7.0
9	11.0	24.2	28.2	3.8	3.8	1.2	4.0
10	12.0	24.1	28.2	4.0	4.3	1.2	2.0
11	4.1	25.4	29.2	6.2	3.8	0.8	0.9
12	4.2	25.0	29.4	3.9	3.3	0.8	1.0
13	7.0	24.4	29.2	4.5	4.4	0.9	1.5
14	5.9	23.8	29.2	4.5	3.8	1.3	0.5
15	6.8	23.9	29.6	4.1	4.5	0.9	1.0

Water samples were passed through a 0.45 μm acetate fiber filter. Acetate fiber filter was first pre-soaked in a 1:1 000 hydrochloric acid solution for 24 h, followed by a pH-neutralizing wash in Milli-Q water. The filtrate was stored at –20℃ for nutrient analysis. The filtrate was used to analyze chemical oxygen demand (COD), nitrite nitrogen (NO_2^--N), nitrate nitrogen (NO_3^--N), ammonia nitrogen (NH_3-N), chlorophyll *a* (Chl *a*), total nitrogen (TN), total phosphorus (TP), and suspended solids (SS) concentrations by nutrient auto-analyzer. pH and dissolved oxygen (DO) were measured directly in the field by pH meter and a Hydrocat CTD probe.

2.3.3 *Fitting analysis*

A large number of studies have demonstrated that the area of *U. prolifera* shows a trend of increasing and then decreasing with time (Sun et al., 2018; Zhang et al., 2022a). This indicates that *U. prolifera* has a discrete distribution, and there may not be a linear relationship between the area and time of the *U. prolifera* outbreak. We found that fitting the area and time of *U. prolifera* outbreak by Gaussian functions could suitably approximate the growth curve of *U. prolifera*. The formula of the Gaussian functions is as follows:

$$f(t) = a \times \mathrm{e}^{-\left(\frac{t-b}{c}\right)^2}, \tag{4}$$

where a, b, and c represent constants. $f(t)$ and t represent the area and time, respectively, of the *U. prolifera* outbreak.

Changes in water quality can affect the concentration of Chl *a* in seawater by influencing the growth of phytoplankton (Zhang et al., 2022b). We explored the relationship between water quality and Chl *a* by MATLAB multiple regression analysis, and established a model between water quality and Chl *a* to explore the effect of water quality changes on Chl *a*. The formula of the multiple regression model is as follows:

$$f(w) = \rho_0 + \rho_1 w_1 + \rho_2 w_2 + \cdots + \rho_n w_n. \tag{5}$$

Equation (5) denotes that the change of n water quality indicators on the linear change of the explanatory variable Chl *a*. ρ_0 represents the constant coefficient, ρ_n represents the regression coefficient, and w_n represents the water quality indicators, including DO, COD, NO_2^--N, NO_3^--N, NH_3-N, Chl *a*, and SS concentrations. To avoid multiple collinearity effects, the water quality indicators were selected by comparing the parameters of the collinearity diagnostic table. Finally, the accuracy of the model was verified by the coefficient of determination. If *R*-squared is greater than 0.6, then the model has some credibility.

3 Results

3.1 *Determination of the dissipation time and location of U. prolifera*

We needed to determine the time and location of *U. prolifera* dissipation to study its impact on the environment. First, we extracted the spatiotemporal distribution of *U. prolifera* in the SYS from 2012 to 2020 based on the GEE platform. We used the Gaussian function to fit the time and area of the *U. prolifera* outbreak based on MATLAB software, determined the dissipation period of the *U. prolifera*, and finally obtained a curve model (Eq. (6)):

$$f(t) = 718.2 \times \mathrm{e}^{-\left(\frac{t-165.7}{18.74}\right)^2}. \tag{6}$$

As illustrated in Fig. 2, the outbreak time and area of the *U. prolifera* had a Gaussian distribution over the most recent nine years. We can see from the Gaussian curve that the process of a *U. prolifera* outbreak is divided into I, II, III, IV, and V stages. These five stages can be divided into discovery, development, outbreak, decline, and disappearance. *Ulva prolifera* entered the growth period in late May and early June. It increased exponentially and reached the outbreak stage in middle and late June. In July, the area of *U. prolifera* began to decline. In August, it began to dissipate and gradually reached the Haiyang shore with the change of environment and the consumption of nutrients.

It has been demonstrated that *U. prolifera* is first detected by remote sensing satellites in northern Jiangsu shoal of China and drifts from southeast to northwest under the action of southeast monsoon and surface currents (Zheng et al., 2022b). A large amount of *U. prolifera* keeps proliferating and gathering together to eventually form the drifting green tide. As shown in Fig. 3, over the most recent nine years, *U. prolifera* dissipation has occurred mainly in Qingdao and Haiyang. The latest study demonstrated that green tide will continue to persist for about half a month past the date of last monitoring by remote sensing images (Li et al., 2021b). The drift and dissipation of *U. prolifera* are continuing during this period, so the green tide that occur in Qingdao will eventually have an impact on Haiyang as well.

3.2 *Effect of U. prolifera dissipation on water quality*

As shown in Figs 2 and 3, the time of *U. prolifera* dissipation is mainly in July and August, and the location of dissipation is mainly in Qingdao and Haiyang of China. We investigated the impact of *U. prolifera* dissipation on the offshore environment based on the field monitoring data from Haiyang in June and August. According to the *Technical Specification for Offshore Environmental Monitoring, Part 3 Offshore Seawater Quality Monitoring of China* (HJ 442.3-2020), we took the mean value of the collected seawater data to analyze the impact of *U. prolifera* dissipation on the surface and deep seawater.

Compared with June, the pH value in the surface seawater de-

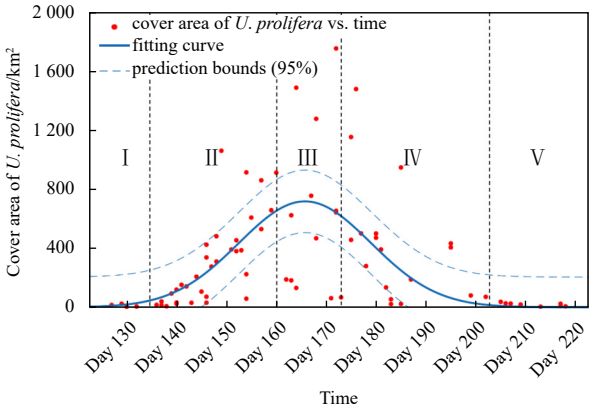

Fig. 2. Fitting analysis of *Ulva prolifera* outbreak time and coverage area in recent nine years. Red points represent the area vs. time of *U. prolifera* outbreak. The solid blue line represents the fitted curve. The blue dashed line represents the forecast interval. The *x*-axis represents the daily ordinal number of a year. May is Day 121 to Day 151, June is Day 152 to Day 181, July is Day 182 to Day 212, and August is Day 213 to Day 243.

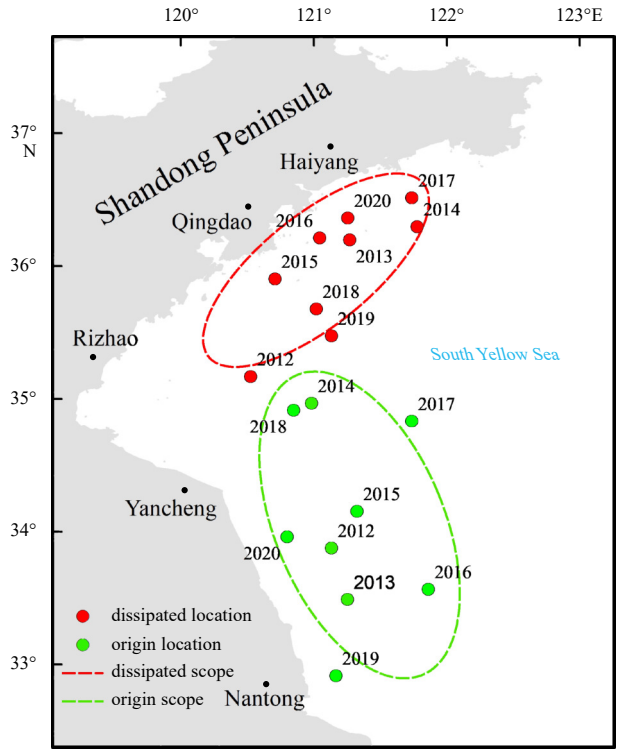

Fig. 3. The origin location and dissipated location of the *Ulva prolifera* in recent nine years. The red and green points represent the dissipated location and the origin location, respectively. The red dashed line and the green dashed line represent the dissipated scope and the origin scope, respectively.

creased by about 0.23 in August after the *U. prolifera* dissipation (Fig. 4). The concentrations of COD, TP, and Chl *a* also decreased to different degrees (0.16 mg/L, 0.006 mg/L and 1.34 mg/L, respectively). The concentrations of DO, NO_2^--N, NO_3^--N, NH_3-N, TN, and SS increased by 0.34 mg/L, 0.01 mg/L, 0.09 mg/L, 0.04 mg/L, 4.33 mg/L, and 6.83 mg/L, respectively. In deep seawater, the concentrations of NH_3-N, DO, NO_2^--N, NO_3^--N, TN, and SS increased by 0.03 mg/L, 0.56 mg/L, 0.01 mg/L, 0.07 mg/L, 4.81 mg/L, and 6.26 mg/L, respectively. The values of COD, pH, Chl *a*, and TP were reduced by 0.04 mg/L, 0.16 mg/L, 0.55 mg/L, and 0.003 mg/L, respectively. These results show that after the *U. prolifera* dissipation the water quality change trend is the same in deep and surface seawater.

Although water quality has the same change trend in different depths of seawater, there may be differences in the extent of change in different depths of seawater. If this occurs, it reflects the extent of the effect of *U. prolifera* dissipation on seawater at different depths. We calculated the average rate of change of 12 water quality indicators in different depths of seawater (Table 2). As illustrated in Table 2, the extent of changes in pH, COD, NO_2^--N, NO_3^--N, NH_3-N, Chl *a*, TP and SS were more significant in surface seawater than in deep water. DO and TN changed more significantly in deep seawater (1.63 and 1.1 times, respectively, more than in surface seawater). This indicates a significant difference in the extent of the effect of *U. prolifera* dissipation on seawater at different depths.

4 Discussions

4.1 *Effects of U. prolifera dissipation on the offshore environment*

Macroalgae play an important role in the climate system and global carbon cycle as coastal blue carbon (Zhao et al., 2021). Numerous studies have shown that *U. prolifera* can absorb inorgan-

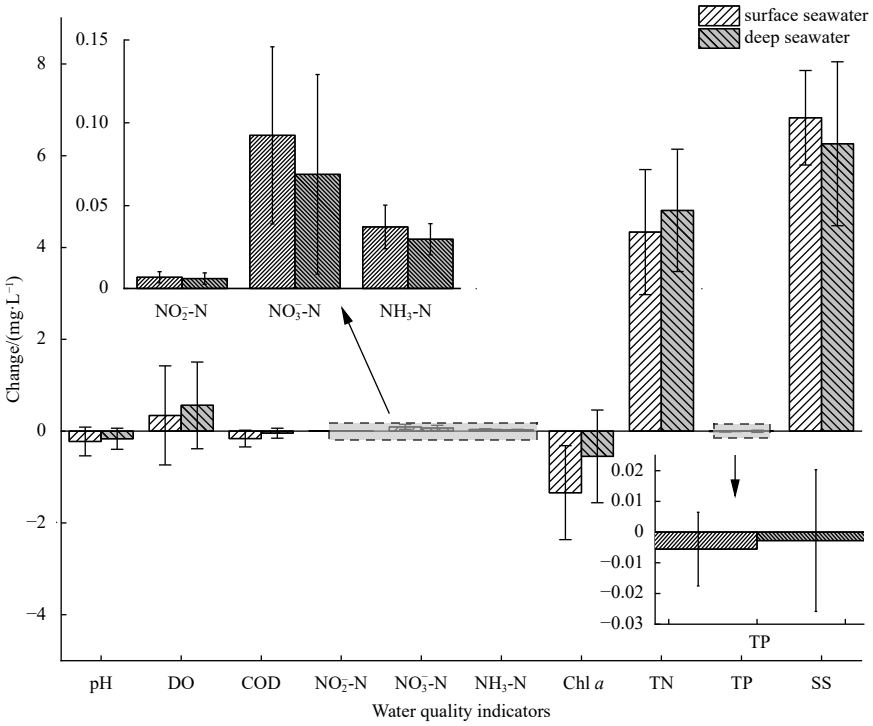

Fig. 4. Changes in water quality concentration after the *Ulva prolifera* dissipation. The *x*-axis represents the water quality indicators; *y*-axis represents the difference between the water quality data in August and June. DO: dissolved oxygen; COD: chemical oxygen demand; NO_2^--N: nitrite nitrogen; NO_3^-: nitrate nitrogen; NH_3-N: ammonia nitrogen; Chl *a*: chlorophyll *a*; TN: total nitrogen; TP: total phosphorus; SS: suspended solid.

Table 2. Average rate of change of water quality concentration at different depths

	pH	DO	COD	NO_2^--N	NO_3^--N	NH_3-N	Chl *a*	TN	TP	SS
Surface seawater	–2.81%	5.20%	–13.61%	691.51%	506.63%	463.56%	–24.48%	893.90%	–26.40%	72.81%
Deep seawater	–2.04%	8.48%	–4.18%	557.45%	460.70%	383.64%	–10.17%	986.68%	–12.63%	69.62%

Note: DO: dissolved oxygen; COD: chemical oxygen demand; NO_2^--N: nitrite nitrogen; NO_3^-: nitrate nitrogen; NH_3-N: ammonia nitrogen; Chl *a*: chlorophyll *a*; TN: total nitrogen; TP: total phosphorus; SS: suspended solid.

ic carbon from seawater through photosynthesis, thus forming a carbon sink (Xu et al., 2012; Deng et al., 2018). *Ulva prolifera* also absorbs a large amount of NO_3^--N, in the growth process, thus forming a nitrogen sink (Zhang et al., 2021b). The growth of *U. prolifera* is a process of absorbing carbon and nitrogen, and dissipation is a process of releasing carbon and nitrogen. It has been demonstrated that the nutrient salts released during *U. prolifera* dissipation are mainly organic (more than 90% of the total nutrient salts), in which the released TN concentration is greater than the standard of eutrophication, reaching 80 μmol/L (Ding, 2014).

The carbon released during the dissipation of *U. prolifera* causes the pH of seawater to decline, which may lead to seawater acidification (Hu et al., 2015). TN, pH, and SS are closely related to carbon in seawater in our water quality indicators. There is a negative correlation between pH and carbon dioxide in seawater. The organic nitrogen in TN and organic compound in SS both contain large amounts of carbon. So, we discuss the effect of *U. prolifera* dissipation on the carbon cycle in seawater from these three indicators. Compared with June, the pH of surface seawater decreased by about 0.23 in August, and the concentrations of TN and SS increased by 4.33 mg/L and 6.83 mg/L, respectively (Fig. 4). In deep seawater, the pH decreased by about 0.16 and the concentrations of TN and SS increased by 4.81 mg/L and 6.26 mg/L, respectively. This indicates that the dissipation of *U. prolifera* released a large amount of carbon into the seawater, resulting in a decline in pH. According to the microbial carbon pump theory (Zhang et al., 2017a, 2017b; Jiao et al., 2018), the dissolved organic carbon (DOC) released during *U. prolifera* decomposition is partially transformed into refractory dissolved organic carbon (RDOC) via microbial metabolism (Zhang et al., 2019). The RDOC is difficult for microorganisms to utilize or degrade, and thus accumulates in the water for a long time, affecting the carbon cycle and water recalcitrant dissolved organic carbon in the ocean (Deng et al., 2018).

The nitrogen released during the decomposition of *U. prolifera* is mainly nitrate and ammonium (Liu et al., 2016). As illustrated in Fig. 4, the concentrations of NO_2^--N, NO_3^--N, and NH_3-N in the surface seawater increased by 0.01 mg/L, 0.09 mg/L, and 0.04 mg/L, respectively, after the dissipation of *U. prolifera*. In deep seawater, the concentrations of NO_2^--N, NO_3^--N, and NH_3-N increased by 0.01 mg/L, 0.07 mg/L, and 0.03 mg/L, respectively. This, to a certain extent, indicates that a large amount of nitrogen was released into seawater during the process of *U. prolifera* decomposition. *Ulva prolifera* decomposition also affects the abundance of bacterial microorganisms in seawater. The abundance of specific bacterial groups such as heterotrophic nitrogen fixing bacteria increased significantly (Zhang et al., 2015). This indicates that *U. prolifera* decomposition affected the nitrogen concentration in seawater through the release of nitrogen and the increase of nitrogen fixing bacteria.

4.2 *Effects of U. prolifera dissipation on phytoplankton*

Ulva prolifera decomposition will release a large number of nutrients, which are absorbed and used by phytoplankton in seawater and will affect the growth and reproduction of phytoplankton (Zhang et al., 2017a). The concentration of Chl *a* is an indicator of phytoplankton biomass. There is a positive correlation between them (Zhang et al., 2022b). The accumulation of phytoplankton on the sea surface will lead to a significant increase in the concentration of Chl *a*. The biomass of phytoplankton is affected by environmental factors, such as temperature and nutrients (Zhang et al., 2022b). Therefore, the effect of water quality change on Chl *a* after *U. prolifera* decomposition can reflect the effect of *U. prolifera* decomposition on phytoplankton.

First, we performed multiple linear regression analyses in MATLAB for the concentration of Chl *a* and the measured water quality data. Then, a linear model was developed to explore the effect of water quality changes on Chl *a*. We found a significant correlation between Chl *a* concentration and pH, DO, NO_3^--N, NH_3-N, and SS after repeated trials. Finally, we built the model as shown in Eq. (7). The *R*-squared of the model is 0.75 and the *p*-value is 1.63×10^{-6}, which is statistically significant. As illustrated in Table 3, Chl *a* was positively correlated with pH and negatively correlated with the concentrations of DO, NO_3^--N, NH_3-N, and SS in this model. This indicates that the changes in pH, DO, NO_3^--N, NH_3-N, and SS will significantly affect the concentration of Chl *a*.

$$\begin{aligned} f(w) =& 10.05w_1w_2 - 91.63w_1w_3 + 159.72w_1w_4 + 0.37w_1w_5 + \\ & 171.33w_2w_3 - 209.52w_2w_4 + 0.05w_2w_5 + 30\,417w_3w_4 + \\ & 29.5w_3w_5 - 3.55w_4w_5 - 27.48w_1^2 - 0.16w_2^2 + \\ & 12\,580w_3^2 - 12\,089w_4^2 - 0.003w_5^2 - 1\,271.9, \end{aligned} \tag{7}$$

where $f(w)$represents the concentration of Chl *a*. w_1, w_2, w_3, w_4, and w_5 represent the values of pH, DO, NO_3^--N, NH_3-N, and SS concentrations, respectively.

As shown in Fig. 4, the decomposition of *U. prolifera* will decrease the pH of seawater. From an ecological point of view, the decrease in pH may lead to seawater acidification, affecting the respiration rate (Gao et al., 2019; Liu et al., 2020), lipid metabolism (Zheng et al., 2009), and nucleic acid metabolism of marine organisms (Franke and Clemmesen, 2011). Seawater acidification may also reduce the abundance of certain phytoplankton species, with cascading effects on the ecosystem (Gao et al., 2021). The *U. prolifera* dissipation leads to the increase of DO, NO_3^--N, NH_3-N, and SS concentrations in the water, which provides phytoplankton with the nutrients required for growth and development. However, excessive nutrients in seawater can

Table 3. Correlation between water quality indicators and Chl *a* concentration

Water quality indicators	Correlation coefficient	*P*
pH	0.48*	0.021
DO	–0.33**	0.002
NO_3^--N	–0.65**	0.001
NH_3-N	–0.68**	0.000
SS	–0.28	0.051

Note: The significance of the correlation coefficient is $^{**}P\leqslant0.01$, $^{*}P\leqslant0.05$. DO: dissolved oxygen; NO_3^--N: nitrate nitrogen; NH_3-N: ammonia nitrogen; SS: suspended solid.

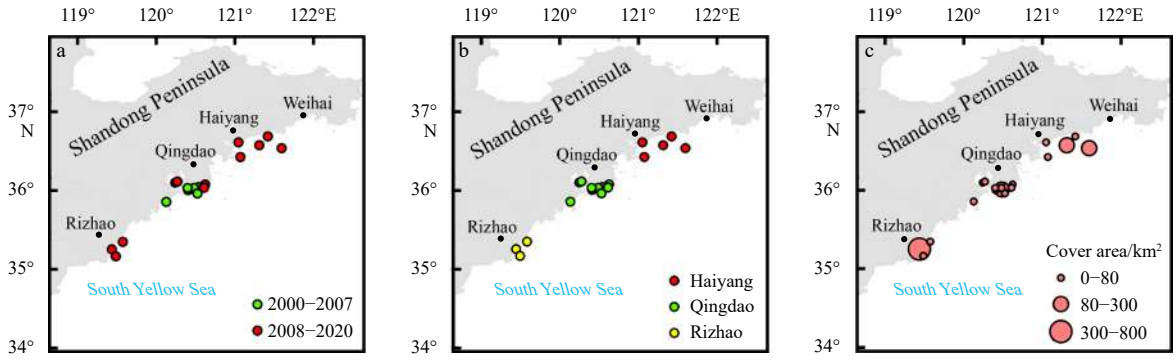

Fig. 5. Spatiotemporal distribution of the red tide in the south of Shandong Peninsula during 2000–2019. Circles with different colors represent the spatial location of red tide. a, b, and c show temporal properties, spatial properties, and outbreak area of the red tide, respectively.

lead to deterioration of water quality. The *U. prolifera* dissipation releases high concentrations of transudates containing abundant nitrogen and phosphorus that may inhibit the growth of some phytoplankton species (Zhang et al., 2019). Meanwhile, allelopathy is one of the most important effects of *U. prolifera* on surrounding organisms. The fatty acid secreted by *U. prolifera* will inhibit the population growth of phytoplankton (Lv et al., 2021). These may be the reasons for the decrease of seawater Chl *a* concentration after the *U. prolifera* dissipation.

During *U. prolifera* dissipation, the concentration of nutrients in seawater is abnormally high and the water quality is poor (Ogawa et al., 2015). Seawater has a certain self-purification ability. The seawater quality will return to its original level within a certain period after the end of the *U. prolifera* dissipation period. The water quality will have a phase suitable for phytoplankton growth during this process. Suitable physicochemical conditions of seawater will promote the growth of phytoplankton. *Ulva prolifera* dissipation releases large amounts of nitrogen into seawater. NH_3-N can promote the growth of planktonic algae, which will easily cause secondary disasters such as red tide (Wang et al., 2007, 2012).

We investigated the red tide around the south of the Shandong Peninsula during 2000–2019. As shown in Fig. 5, a total of 19 large-scale red tide disasters occurred in the south of the Shandong Peninsula over the most recent 20 years. There were 13 red tide disasters after the 2008 Qingdao green tide disaster. Five red tide disasters occurred in Haiyang after 2008. The area of the 2008 red tide disaster in Haiyang reached 300 km^2. The red tide occurring in Haiyang are caused by phytoplankton, such as *Noctiluca scintillans*, *Chattonella marina*, and *Gnoyaulax spinifera* (Zhou et al., 2022). This indicates that the green tide in Qingdao may have some correlations with the red tide in Haiyang. To a certain extent, this reveals the relationship between green tide and red tide: the nutrients in seawater returns to suitable levels after the *U. prolifera* dissipation, which for a while will promote the growth of phytoplankton and may trigger red tide. This is also consistent with the results of laboratory simulation and field investigations (Wang et al., 2012; Kong et al., 2018).

5 Conclusions

We explored the effects of *U. prolifera* dissipation on the offshore environment based on data from the GEE platform, MATLAB fitting analysis, and measured seawater data. The results of the study show that the *U. prolifera* dissipates in Haiyang in July and August every year and has an impact on the offshore environment. By measuring the water quality data from Haiyang, we found that the dissipation of *U. prolifera* leads to different changes in water quality at different depths. The dissipation of *U. prolifera* can lead to changes in water quality and trigger secondary disasters. Our results show that the dissipation of *U. prolifera* releases large amounts of carbon and nitrogen into seawate. With the recovery of water quality, the large amount of nitrogen present in seawater will promote the growth of phytoplankton, which may cause secondary disasters such as red tide. In the future, we will further explore the pattern of *U. prolifera* outbreak and the impact of *U. prolifera* dissipation on the offshore environment to provide a theoretical basis for the prevention and control of green tide.

References

Chen Jing, Li Hongmei, Zhang Zenghui, et al. 2020. DOC dynamics and bacterial community succession during long-term degradation of *Ulva prolifera* and their implications for the legacy effect of green tides on refractory DOC pool in seawater. Water Research, 185: 116268, doi: 10.1016/j.watres.2020.116268

Deng Xue, Liu Tao, Liu Chunying, et al. 2018. Effects of *Ulva prolifera* blooms on the carbonate system in the coastal waters of Qingdao. Marine Ecology Progress Series, 605: 73–86, doi: 10.3354/meps12739

Ding Yuemin. 2014. Impacts of *Ulva* (*Enteromorpha*) *prolifera* in the green tide on the Yellow Sea ecological environment-implications from migration and transformation of biogenic elements (in Chinese)[dissertation]. Qingdao: Institute of Oceanology, Chinese Academy of Sciences

Feng Lina, Zhang Haibo, Sun Yuyan, et al. 2020. On nutrient releases from the decomposition of *Ulva prolifera* green tide and their impacts on nearshore seawaters in the southern Yellow Sea. Haiyang Xuebao (in Chinese), 42(8): 59–68

Franke A, Clemmesen C. 2011. Effect of ocean acidification on early life stages of Atlantic herring (*Clupea harengus* L.). Biogeosciences, 8(12): 3697–3707, doi: 10.5194/bg-8-3697-2011

Gao Guang, Gao Qi, Bao Menglin, et al. 2019. Nitrogen availability modulates the effects of ocean acidification on biomass yield and food quality of a marine crop *Pyropia yezoensis*. Food Chemistry, 271: 623–629, doi: 10.1016/j.foodchem.2018.07.090

Gao Guang, Zhao Xin, Jiang Meijia, et al. 2021. Impacts of marine heatwaves on algal structure and carbon sequestration in conjunction with ocean warming and acidification. Frontiers in Marine Science, 8: 758651, doi: 10.3389/fmars.2021.758651

Hao Binfei, Yang Hong, Ma Mingguo, et al. 2020. Variation in land use and land surface parameters in the three gorges reservoir catchment based on Google Earth Engine. Resources and Environment in the Yangtze Basin (in Chinese), 29(6): 1343–1355

Hu Yubin, Liu Chunying, Yang Guipeng, et al. 2015. The response of the carbonate system to a green algal bloom during the post-bloom period in the southern Yellow Sea. Continental Shelf Re-

search, 94: 1–7, doi: 10.1016/j.csr.2014.12.006
Jiao Nianzhi, Cai Ruanhong, Zheng Qiang, et al. 2018. Unveiling the enigma of refractory carbon in the ocean. National Science Review, 5(4): 459–463, doi: 10.1093/nsr/nwy020
Kong Fanzhou, Jiang Peng, Wei Chuanjie, et al. 2018. Co-occurence of green tide, golden tide and red tides along the 35°N transect in the yellow sea during spring and summer in 2017. Oceanologia et Limnologia Sinica (in Chinese), 49(5): 1021–1030
Kwon H K, Kang H, Oh Y H, et al. 2017. Green tide development associated with submarine groundwater discharge in a coastal harbor, Jeju, Korea. Scientific Reports, 7(1): 6325, doi: 10.1038/s41598-017-06711-0
Li Dongxue, Gao Zhiqiang, Song Debin. 2021a. Analysis of environmental factors affecting the large-scale long-term sequence of green tide outbreaks in the Yellow Sea. Estuarine, Coastal and Shelf Science, 260: 107504, doi: 10.1016/j.ecss.2021.107504
Li Dongxue, Gao Zhiqiang, Xu Fuxiang. 2021b. Research on the dissipation of green tide and its influencing factors in the Yellow Sea based on Google Earth Engine. Marine Pollution Bulletin, 172: 112801, doi: 10.1016/j.marpolbul.2021.112801
Li Binghan, Liu Chunying, Deng Xue, et al. 2021c. Responses of the marine carbonate system to a green tide: a case study of an *Ulva prolifera* bloom in Qingdao coastal waters. Harmful Algae, 110: 102133, doi: 10.1016/j.hal.2021.102133
Liu Dongyan, Keesing J K, Xing Qianguo, et al. 2009. World's largest macroalgal bloom caused by expansion of seaweed aquaculture in China. Marine Pollution Bulletin, 58(6): 888–895, doi: 10.1016/j.marpolbul.2009.01.013
Liu Xiangqing, Wang Zongling, Xin Ming, et al. 2016. Study on process of nutrient release during the decay of *Ulva Prolifera*. Marine Environmental Science (in Chinese), 35(6): 801–805, 813
Liu Chunxiang, Zou Dinghui, Liu Zhiwei, et al. 2020. Ocean warming alters the responses to eutrophication in a commercially farmed seaweed, *Gracilariopsis lemaneiformis*. Hydrobiologia, 847(3): 879–893, doi: 10.1007/s10750-019-04148-2
Lv Mengchen, Yuan Mengqi, Wang Ying, et al. 2021. Allelopathic effects of *Ulva linza* on marine phytoplankton and identification of the allelochemicals. Environmental Science and Pollution Research, 28(33): 45714–45723, doi: 10.1007/s11356-021-13734-8
Nguyen U N T, Pham L T H, Dang T D. 2020. Correction to: an automatic water detection approach using Landsat 8 OLI and Google Earth Engine cloud computing to map lakes and reservoirs in New Zealand. Environmental Monitoring and Assessment, 192(9): 616, doi: 10.1007/s10661-020-08581-y
Ogawa T, Ohki K, Kamiya M. 2015. High heterozygosity and phenotypic variation of zoids in apomictic *Ulva prolifera* (Ulvophyceae) from brackish environments. Aquatic Botany, 120: 185–192, doi: 10.1016/j.aquabot.2014.05.015
Schreyers L, van Emmerik T, Biermann L, et al. 2021. Spotting green tides over brittany from space: three decades of monitoring with landsat imagery. Remote Sensing, 13(8): 1408, doi: 10.3390/rs13081408
Sun Xiao, Wu Mengquan, Xing Qianguo, et al. 2018. Spatio-temporal patterns of *Ulva prolifera* blooms and the corresponding influence on chlorophyll-*a* concentration in the southern Yellow Sea, China. Science of the Total Environment, 640–641: 807–820, doi: 10.1016/j.scitotenv.2018.05.378
Wang Bin, Wu Lei. 2021. Numerical study on the massive outbreak of the *Ulva prolifera* green tides in the southwestern Yellow Sea in 2021. Journal of Marine Science and Engineering, 9(11): 1167, doi: 10.3390/jmse9111167
Wang You, Yu Zhiming, Song Xiuxian, et al. 2007. Effects of macroalgae *Ulva pertusa* (Chlorophyta) and *Gracilaria lemaneiformis* (Rhodophyta) on growth of four species of bloom-forming dinoflagellates. Aquatic Botany, 86(2): 139–147, doi: 10.1016/j.aquabot.2006.09.013
Wang Chao, Yu Rencheng, Zhou Mingjiang. 2011. Acute toxicity of live and decomposing green alga *Ulva* (*Enteromorpha*) *prolifera* to abalone *Haliotis discus hannai*. Chinese Journal of Oceanology and Limnology, 29(3): 541–546, doi: 10.1007/s00343-011-0126-3
Wang Chao, Yu Rencheng, Zhou Mingjiang. 2012. Effects of the decomposing green macroalga *Ulva* (*Enteromorpha*) *prolifera* on the growth of four red-tide species. Harmful Algae, 16: 12–19, doi: 10.1016/j.hal.2011.12.007
Wu Mengquan, Guo Hao, Zhang Anding, et al. 2014. Research on the characteristics of *Ulva Prolifera* in Shandong Peninsula during 2008–2012 based on MODIS data. Spectroscopy and Spectral Analysis (in Chinese), 34(5): 1312–1318
Xing Qianguo, Hu Chuanmin, Tang Danling, et al. 2015. World's largest macroalgal blooms altered phytoplankton biomass in summer in the Yellow Sea: satellite observations. Remote Sensing, 7(9): 12297–12313, doi: 10.3390/rs70912297
Xu Jianfang, Fan Xiao, Zhang Xiaowen, et al. 2012. Evidence of coexistence of C_3 and C_4 photosynthetic pathways in a green-tide-forming alga, *Ulva prolifera*. PLoS ONE, 7(5): e37438, doi: 10.1371/journal.pone.0037438
Yin Qi, Liu Maolin, Cheng Junyi, et al. 2019. Mapping paddy rice planting area in northeastern China using spatiotemporal data fusion and phenology-based method. Remote Sensing, 11(14): 1699, doi: 10.3390/rs11141699
Zhang Baowei, Guo Jianzhong, Li Ziwei, et al. 2022a. Identifying the spatio-temporal variations of *Ulva prolifera* disasters in all life cycle. Journal of Water and Climate Change, 13(2): 629–644, doi: 10.2166/wcc.2021.424
Zhang Yongyu, He Peimin, Li Hongmei, et al. 2019. *Ulva prolifera* green-tide outbreaks and their environmental impact in the Yellow Sea, China. National Science Review, 6(4): 825–838, doi: 10.1093/nsr/nwz026
Zhang Xiaoli, Song Yanjing, Liu Dongyan, et al. 2015. Macroalgal blooms favor heterotrophic diazotrophic bacteria in nitrogen-rich and phosphorus-limited coastal surface waters in the Yellow Sea. Estuarine, Coastal and Shelf Science, 163: 75–81, doi: 10.1016/j.ecss.2014.12.015
Zhang Guangzong, Wu Mengquan, Sun Xiao, et al. 2018. The interannual drift and driven force of *Ulva prolifera* bloom in the southern Yellow Sea. Oceanologia et Limnologia Sinica (in Chinese), 49(5): 1084–1093
Zhang Guangzong, Wu Mengquan, Wei Juan, et al. 2021a. Adaptive threshold model in Google Earth Engine: a case study of *Ulva prolifera* extraction in the South Yellow Sea, China. Remote Sensing, 13(16): 3240, doi: 10.3390/rs13163240
Zhang Guangzong, Wu Mengquan, Zhang Anding, et al. 2020. Influence of sea surface temperature on outbreak of *Ulva prolifera* in the southern Yellow Sea, China. Chinese Geographical Science, 30(4): 631–642, doi: 10.1007/s11769-020-1129-9
Zhang Guangzong, Wu Mengquan, Zhou Min, et al. 2022b. The seasonal dissipation of *Ulva prolifera* and its effects on environmental factors: based on remote sensing images and field monitoring data. Geocarto International, 37(3): 860–878, doi: 10.1080/10106049.2020.1745301
Zhang Pengyan, Xin Yu, Zhong Xiaosong, et al. 2021b. Integrated effects of *Ulva prolifera* bloom and decay on nutrients inventory and cycling in marginal sea of China. Chemosphere, 264: 128389, doi: 10.1016/j.chemosphere.2020.128389
Zhang Hailong, Yuan Yibo, Xu Yongjiu, et al. 2021c. Remote sensing method for detecting green tide using HJ-CCD top-of-atmosphere reflectance. International Journal of Applied Earth Observation and Geoinformation, 102: 102371, doi: 10.1016/j.jag.2021.102371
Zhang Yongyu, Zhang Jihong, Liang Yantao, et al. 2017a. Carbon sequestration processes and mechanisms in coastal mariculture environments in China. Science China: Earth Sciences, 60(12): 2097–2107, doi: 10.1007/s11430-017-9148-7
Zhang Yao, Zhao Meixun, Cui Qiu, et al. 2017b. Processes of coastal ecosystem carbon sequestration and approaches for increasing carbon sink. Science China: Earth Sciences, 60(5): 809–820, doi: 10.1007/s11430-016-9010-9
Zhao Peng, Jiang Shu, Shi Jianbin. 2021. Blue carbon in the special report on the ocean and cryosphere in a Changing climate and its impacts. Marine Sciences (in Chinese), 45(2): 137–143

Zheng Xiaozhong, Ding Zhaokun, Xu Youqing, et al. 2009. Physiological roles of fatty acyl desaturases and elongases in marine fish: characterisation of cDNAs of fatty acyl Δ6 desaturase and *elovl5* elongase of cobia (*Rachycentron canadum*). Aquaculture, 290(1–2): 122–131, doi: 10.1016/j.aquaculture.2009.02.010

Zheng Longxiao, Wu Mengquan, Cui Yating, et al. 2022a. What causes the great green tide disaster in the South Yellow Sea of China in 2021?. Ecological Indicators, 140: 108988, doi: 10.1016/j.ecolind.2022.108988

Zheng Longxiao, Wu Mengquan, Zhou Min, et al. 2022b. Spatiotemporal distribution and influencing factors of *Ulva prolifera* and *Sargassum* and their coexistence in the South Yellow Sea, China. Journal of Oceanology and Limnology, 40(3): 1070–1084, doi: 10.1007/s00343-021-1040-y

Zhou Min, Wu Mengquan, Zhao Lianjie, et al. 2022. Temporal and spatial distributions and influencing factors of HABs outbreaks around the north of Shandong Peninsula during 2000–2019: based on remote sensing images and field monitoring data. Geocarto International, 37(25): 8440–8455, doi: 10.1080/10106049.2021.2002425